

# 1        **Sucrose phosphorylase from *Alteromonas mediterranea*: structural** 2        **insight into the regioselective $\alpha$ -glucosylation of (+)-catechin**

3    Marine Goux<sup>a,c</sup>, Marie Demonceaux<sup>a,d</sup>, Johann Hendrickx<sup>a,e</sup>, Claude Solleux<sup>a</sup>, Emilie Lormeau<sup>a</sup>,  
4    Folmer Fredslund<sup>b,f</sup>, David Tezé<sup>b,g</sup>, Bernard Offmann<sup>a,h,j</sup> and Corinne André-Miral<sup>a,i,j</sup>

5

6    <sup>a</sup> Nantes Université, CNRS, US2B, UMR 6286, F-44000, Nantes, France

7    <sup>b</sup> DTU Biosustain, Technical University of Denmark, DK-2800 Kgs. Lyngby, Denmark

8    <sup>c</sup> ORCID number: 0000-0002-8350-4102, e-mail : [marine.goux-huet@univ-nantes.fr](mailto:marine.goux-huet@univ-nantes.fr)

9    <sup>d</sup> ORCID number: 0000-0002-6090-4007, e-mail : [marie.demonceaux@univ-nantes.fr](mailto:marie.demonceaux@univ-nantes.fr)

10    <sup>e</sup> ORCID number: 0000-0002-3988-2747, e-mail : [johann.hendrickx@univ-nantes.fr](mailto:johann.hendrickx@univ-nantes.fr)

11    <sup>f</sup> ORCID number: 0000-0003-0881-1927, e-mail : [folf@biosustain.dtu.dk](mailto:folf@biosustain.dtu.dk)

12    <sup>g</sup> ORCID number: 0000-0002-6865-6108, e-mail : [datez@biosustain.dtu.dk](mailto:datez@biosustain.dtu.dk)

13    <sup>h</sup> ORCID number: 0000-0002-6845-5883, e-mail : [bernard.offmann@univ-nantes.fr](mailto:bernard.offmann@univ-nantes.fr)

14    <sup>i</sup> ORCID number: 0000-0002-3378-2331, e-mail : [corinne.miral@univ-nantes.fr](mailto:corinne.miral@univ-nantes.fr)

15    <sup>j</sup> Corresponding authors: Corinne André-Miral and Bernard Offmann

## 16    **Abstract**

17    Flavonoids glycosylation at different positions is paramount to solubility and modulation of  
18    bioactivities. Sucrose phosphorylases, through transglycosylation reactions, are interesting  
19    enzymes that can transfer glucose from sucrose, the donor substrate, onto polyphenols to form  
20    glycoconjugates. Here, we report for the first time the structural and enzymatic properties of  
21    sucrose phosphorylase from the marine bacteria *Alteromonas mediterranea* (AmSP). We  
22    characterized and investigated the transglucosylation capacity of two new variants of the enzyme  
23    on (+)-catechin and their propensity to catalyse its regioselective glucosylation. AmSP-Q353F and

24 AmSP-P140D were shown to catalyse the regiospecific glucosylation of (+)-catechin using sucrose  
25 as donor substrate. While AmSP-WT was devoid of synthetic activity, each of its two single mutant  
26 provided high yields of specific regioisomers: 89% of (+)-catechin-4'-O- $\alpha$ -D-glucopyranoside (CAT-  
27 4') for AmSP-P140D and 92% of (+)-catechin-3'-O- $\alpha$ -D-glucopyranoside (CAT-3') for AmSP-Q353F.  
28 The novel compound CAT-4' was fully characterized by NMR and mass spectrometry. We used  
29 molecular docking simulations on structural models of the glucosyl-enzyme intermediate to  
30 explain this regioselectivity. We showed that AmSP-P140D preferentially binds (+)-catechin in a  
31 mode that favours glucosylation on its hydroxyl group in position 4' (OH-4') while the binding  
32 mode of the flavonoid in AmSP-Q353F favoured glucosylation on its hydroxyl group in position 3'  
33 (OH-3').

34 Keywords: marine microbial enzymes, regioselectivity, biocatalysis, (+)-catechin, sucrose-  
35 phosphorylase, *Alteromonas mediterranea*

## 36 1. Introduction

37 Oceans cover more than 70% of Earth's surface and provides a unique environment to marine  
38 bacteria (*i.e.* high salinity, high pressure, low temperature and special lighting conditions). For  
39 decades, enzymes have been isolated and purified from terrestrial microorganisms, animals and  
40 plants. With the advent of biotechnology, there has been a growing interest and demand for  
41 enzymes with novel properties and robust biocatalysts. Due to its complexity, the marine  
42 environment represents a great opportunity for exploration of new enzymes and molecules [1, 2].  
43 Marine enzymes are capable of being active under extreme conditions, which provide  
44 competitiveness and efficiency to different industrial processes [3, 4]. Among those, sucrose-  
45 phosphorylases (SPs) from the Glycoside Hydrolase family 13 subfamily 18 (GH13\_18, EC 2.4.1.7)  
46 attract biotechnological interest as biocatalysts. Requiring only a cheap and abundant donor, SPs  
47 can perform transglucosylation reaction by transferring glucose from sucrose to an acceptor to

48 yield  $\alpha$ -glucosylated products with a retaining mechanism via a  $\beta$ -glucosyl-enzyme intermediate.  
49 Particularly, *Bifidobacterium adolescentis* SP (*BaSP*-WT) and its mutants have been studied for  
50 biocatalytic synthesis of rare disaccharides [5, 6] and  $\alpha$ -glucosylation of polyphenols [7, 8, 9, 10].  
51 To date, the only documented structures of sucrose phosphorylase in the literature are from  
52 *Bifidobacterium adolescentis* [11]. Other SPs, from *Leuconostoc mesenteroides*, *Streptococcus*  
53 *mutans*, *Lactobacillus acidophilus* and *Thermoanaerobacterium thermosaccharolyticum*, have also  
54 been studied for the glucosylation of phenolic compounds [12, 13, 14]. Glucosylation of this type  
55 of molecules increases their solubility in water and their bioavailability in health, nutraceuticals  
56 and cosmetics applications [15, 16]. Controlling the regioselectivity of this glucosylation is also at  
57 stake for the synthesis of new compounds. We recently documented the activity of two variants of  
58 *BaSP*-WT with respect to their ability to transfer regioselectively a glucose moiety onto (+)-  
59 catechin as an acceptor substrate [10]. *BaSP*-Q345F and *BaSP*-P134D/Q345F glucosylated (+)-  
60 catechin on hydroxyl groups in position 3' (OH-3') and 5 (OH-5) with obtainment of three  
61 glucosylated regioisomers: (+)-catechin-3'-O- $\alpha$ -D-glucopyranoside (CAT-3'), (+)-catechin-5-O- $\alpha$ -D-  
62 glucopyranoside (CAT-5) and (+)-catechin-3',5-O- $\alpha$ -D-diglucopyranoside (CAT-3',5), with a ratio of  
63 51:25:24 for *BaSP*-Q345F and 82:9:9 for *BaSP*-P134D/Q345F.  
64 *Alteromonas mediterranea*, also known as *Alteromonas macleodii* "Deep Ecotype" or AltDE, is an  
65 aerobic Gram-negative and mesophilic marine bacterium from the genus of *Proteobacteria* which  
66 was first isolated at a depth of 1000 m in the Eastern Mediterranean Sea in 2005 [17, 18, 19]. Wild  
67 type form of *AmSP* (*AmSP*-WT) shares 52% of global sequence identity with *BaSP*-WT. Sequence  
68 alignments revealed that both enzymes possess highly conserved regions corresponding to the  
69 loop A (*BaSP*-WT: <sup>336</sup>AAASNLDLYQ<sup>345</sup>, *AmSP*-WT: <sup>344</sup>AAASNLDLYQ<sup>353</sup>) and loop B (*BaSP*-WT:  
70 <sup>132</sup>YRPRP<sup>136</sup>, *AmSP*-WT: <sup>138</sup>FRPRP<sup>142</sup>) of the catalytic site [20]. In a preliminary screening using  
71 homology modelling and molecular docking, we identified that the catalytic cavity of the glucosyl-  
72 intermediate of *AmSP*-WT could potentially host a polyphenolic acceptor compound like (+)-

73 catechin. We thus characterized *AmSP*-WT from a structural and functional perspective. Towards  
74 this end, the crystallographic structure of *AmSP*-WT was for the first time recently determined  
75 [Goux *et al.*, in preparation]. In the present work, we further analysed the structural features of  
76 *AmSP*-WT and investigated the enzymatic properties of two variants of the enzyme towards their  
77 propensity to catalyse the regioselective transglucosylation of (+)-catechin. P140D and Q353F  
78 mutations, homologous to mutations P134D and Q345F of *BaSP*-WT, displayed a single transfer  
79 reaction product for each enzyme: (+)-catechin-4'-O- $\alpha$ -D-glucopyranoside (CAT-4') for *AmSP*-  
80 P140D and CAT-3' for *AmSP*-Q353F. To explain the striking enzymatic activities of those variants,  
81 we provide in-depth structural insights by docking simulations and modelling. Our results  
82 interestingly broaden the available chemo-enzymatic synthetic tools for the efficient regioselective  
83  $\alpha$ -glucosylation of polyphenols.

## 84 2. Materials and methods

### 85 2.1. Vector construction and proteins

86 *AmSP*-WT and its variants were expressed as C-terminally hexahistidine-tagged proteins, allowing  
87 affinity purification by standard protocols. *AmSP*-WT gene (UniProt: S5AE64\_9ALTE) was ordered  
88 from Genscript already cloned in a pET28b vector. *E. coli* BL21(DE3) competent cells (Novagen)  
89 were transformed with pET28b\_ *AmSP*-WT. Clones were selected using LB-agar medium  
90 supplemented with 25  $\mu$ g/mL kanamycin and confirmed by Sanger sequencing (Eurofins  
91 Genomics). Variants *AmSP*-P140D, *AmSP*-Q353F and *AmSP*-P140D/Q353F were obtained by site-  
92 directed mutagenesis. Proteins were produced, purified and characterized as previously described  
93 [10].

## 94 2.2. *Transglucosylation studies*

95 Reactions were carried out in 50 mM 3-morpholinopropane-1-sulfonic acid (MOPS)-NaOH solution  
96 at pH 8.0 in a total volume of 1 mL. Reaction mixture containing 10 mM (+)-catechin in DMSO (1  
97 eq., 100  $\mu$ L), 10% DMSO (100  $\mu$ L, (v/v)), 80 mM sucrose in H<sub>2</sub>O (8 eq., 100  $\mu$ L) was incubated with a  
98 final concentration of 10  $\mu$ M of purified enzyme at 25°C under slight agitation. Enzymatic synthesis  
99 was monitored by thin layer chromatography (TLC) for 48h. TLC plates were developed in solution  
100 composed of ethyl acetate/methanol/cyclohexane/water (6.75:1.35:1:0.9, v/v/v/v) with 0.1%  
101 formic acid (v/v). Products were visualized using a UV lamp at 254 nm and revealed with vanillin-  
102 sulphuric acid reagent.

## 103 2.3. *Purification and analysis of glucosylated (+)-catechin*

104 After centrifugation (12 000 x g, 20 min), 10  $\mu$ L of the supernatant was analysed by analytical HPLC  
105 at 280 nm on a C-18 column (Interchim, 5  $\mu$ m, 250 x 4.6 mm, US5C18HQ-250/046) with an  
106 isocratic flow of 80% H<sub>2</sub>O (v/v), 0.1% formic acid (v/v) and 20% MeOH (v/v), 0.1% formic acid (v/v)  
107 for 20 min. Then, remaining supernatant was purified by HPLC at 280 nm on a C-18 column  
108 (Interchim, 5  $\mu$ m, 250 x 21.2 mm, US5C18HQ-250/212) with a gradient system (solvent A: H<sub>2</sub>O  
109 HCOOH 0.1%; solvent B: MeOH, HCOOH 0.1%; t<sub>0</sub> min = 70/30, t<sub>10</sub> min = 70/30, t<sub>70</sub> min = 10/90).  
110 Products were identified by NMR <sup>1</sup>H and <sup>13</sup>C in MeOD or DMSO-d<sub>6</sub> (400 Hz, 256 scans). For  
111 characterization of CAT-3', CAT-5 and CAT-3',5, see [10].

## 112 2.4. *Molecular modelling of variants of AmSP-WT*

113 Glucosyl-enzyme intermediate 3D-models were built for AmSP-Q353F and AmSP-P140D using the  
114 following procedure and the Rosetta software [22]. Glucosylated-aspartyl 192 residue from chain  
115 A of crystal structure of BaSP-WT (PDB: 2GDV-A) was inserted into the crystal structure AmSP-WT

116 (PDB: 7ZNP) that served as initial template for both variants. As this glucosylated aspartyl is a non-  
117 standard residue, it was absent from the database of the Rosetta software. Using Pymol3, the  
118 initial coordinates of this modified residue were retrieved. While this residue (D192) and the  
119 glucose moiety (BGC) are covalently linked in the crystal structure, the Pymol software considered  
120 them as two distinct residues. Thus, they were merged them into a single non-standard residue,  
121 which was called with a new ID, DGC. Associated charges and rotamers were calculated for this  
122 new residue using the Rosetta software. All those data were merged a single file that we added  
123 into the Rosetta database (Section 2.7).

124 With the DGC residue ready to be used, glucosyl-intermediates were built for the two variants of  
125 AmSP-WT. From the crystal structure (PDB: 7ZNP), using Rosetta the native aspartyl residue in  
126 position 203 was mutated by the glucosylated-aspartyl DGC residue together with either the  
127 P140D or Q353F mutation. For each variant (AmSP-Q353F or AmSP-P140D), a sample of 50  
128 conformers was generated thanks to the program Backrub from Rosetta suite, with 10 000 tries. In  
129 parallel, 12 conformers of (+)-catechin were also generated using the Mercury software (CCDC)  
130 [23] from the crystal structure OZIDOR of (+)-catechin.

### 131 2.5. Docking analysis of binding mode of (+)-catechin in the catalytic pocket

132 All docking experiments were performed with AutoDock Vina using the glucosyl-intermediates and  
133 (+)-catechin conformers built above. Docking perimeter was limited to the residues of the active  
134 site of the enzyme. Each of the 12 conformers of (+)-catechin were docked on every conformer of  
135 the two variants. This amounts to a total of 600 (50x12) docking experiments for each variant of  
136 the enzyme. Only the productive poses that could lead to a glucosylation of (+)-catechin were  
137 selected. To do so, docking poses were filtered using the following distance constraints: distances  
138 within 3.0 Å between any oxygen of (+)-catechin and the anomeric carbon atom C1 of the glucosyl  
139 moiety were assessed. Docking scores were compiled for these productive poses and compared

140 between the two variants. R statistics software package was used to perform the boxplots  
141 analysis.

### 142 3. Results

#### 143 3.1. *Highly conserved structural features and potential activity of AmSP-WT*

144 Through structural comparison of *BaSP*-WT (PDB: 1R7A, 2GDV), *BaSP*-Q345F (PDB: 5C8B), and our  
145 recently determined structure of *AmSP*-WT (PDB: 7ZNP), we identified the conserved residues  
146 likely involved in the reaction mechanism and potential substrate interactions (Table S1). The -1  
147 subsite of SPs, also called donor site, has an optimal topology for binding glucose and is conserved  
148 between *BaSP*-WT and *AmSP*-WT (Figure 1). The configuration of the two catalytic residues  
149 involved in the reaction mechanism are also almost identical (Figure 1A, in blue): a glutamyl  
150 residue acts as a general acid/base catalyst (E243 for *AmSP*-WT and E232 for *BaSP*-WT) and an  
151 aspartyl residue performs the nucleophilic attack (D203 for *AmSP*-WT and D192 for *BaSP*-WT). The  
152 third member of the catalytic triad (D301 for *AmSP*-WT and D290 for *BaSP*-WT) stabilises the  
153 transition state with a strong hydrogen bond and presents also an identical configuration in the  
154 catalytic site. The structural elements that were shown to stabilize the glucosyl moiety in *BaSP*-WT  
155 by non-polar contacts between a hydrophobic platform (F53/F156 for *BaSP*-WT) and the  
156 hydrophobic C3-C4-C5 part of glucose are also conserved in *AmSP*-WT (F56/F167). The acceptor or  
157 +1 site of SPs is mainly shaped by two highly dynamic loops (Figure S1), which were shown to  
158 adopt different conformations based on the progress of the reaction mechanism: one  
159 conformation is the “donor binding mode” or closed conformation and the other is the “acceptor  
160 binding mode” or open conformation where an arginyl residue (R135 in *BaSP*-WT) is thought to  
161 enable the enzyme to outcompete water as an acceptor through strong electrostatic interactions.  
162 When we compare the apoenzyme of *BaSP*-WT (PDB: 1R7A) with our newly obtained apoenzyme

163 of AmSP-WT (PDB: 7ZNP), a striking difference in the positioning of loop A is noticed. The enzyme  
164 has already an opened conformation and is in the “acceptor binding mode” with Y352 residue  
165 pointing inside the active site (Figure 1, in magenta) and R141 pointing outside (Figure 1, in  
166 orange). This open conformation was also observed for BaSP-WT crystallized with the end-product  
167 of the reaction after hydrolysis of glucose (PDB: 2GDV, chain B). Moreover, crucial conserved  
168 residues involved in binding of both phosphate and fructose, Y196 and H234 for BaSP-WT vs. Y207  
169 and H245 for AmSP-WT, are in the same conformational positions thus allowing sucrose  
170 phosphorylase activity (Figure 1B, in cyan)[21]. In BaSP-WT, Y132 is located at the entrance of the  
171 active site and contributes to sucrose specificity thanks to hydrophobic interactions with Y196 and  
172 F206. In AmSP-WT, the aromatic structure is conserved with the replacement of the tyrosinyl  
173 moiety by a phenylalanyl residue in position 138 (Figure 1B, in orange).

### 174 3.2. *Determination of the apparent kinetic parameters*

175 Interestingly, the P140D and Q353F mutations did not alter the enzyme stability, as evidenced by  
176 unchanged melting temperature ( $T_m$ ) of 43°C (Figure S2, Table S2). The apparent kinetic  
177 parameters for sucrose at 25°C with and without 20% DMSO were determined. For each condition,  
178 variants present a decrease of catalytic efficiency towards sucrose of one order of magnitude  
179 compared to the wild-type (Table 1). A loss in specificity for sucrose was observed for AmSP-  
180 Q353F with an increasing of the  $K_m$  value from 1 mM for AmSP-WT to 5 mM for AmSP-Q353F. With  
181 DMSO, AmSP-P140D displayed a higher specificity for sucrose with a  $K_m$  value similar to the wild-  
182 type, resulting in a catalytic efficiency increasing by almost 2-fold compared to the results  
183 obtained without DMSO. For AmSP-Q353F, with 20% of DMSO, we observed no change for the  
184 specificity for sucrose and the turnover number.



### 185 3.3. (+)-catechin transglucosylation studies

186 We assessed the ability of SPs to transfer a glucose moiety from sucrose to (+)-catechin at 25°C  
187 after 24h under agitation. Observed products were purified by preparative HPLC and analysed by  
188 NMR. AmSP-P140D and AmSP-Q353F, catalyse efficiently the synthesis of two different  
189 regioisomers of (+)-catechin glucoside: AmSP-P140D glucosylate mostly the hydroxyl groups in  
190 position 4' (OH-4') while AmSP-Q353F glucosylate the OH-3' position (Figure S5, Table S4). We  
191 monitored the synthesis of glucosylated (+)-catechin products during 24h by HPLC to determine  
192 conversion yields and proportion of regioisomers (Figure 2, Table 2). Interestingly, the main  
193 product formed with AmSP-P140D was CAT-4' with a relative proportion of 89% while the main  
194 product formed with AmSP-Q353F was CAT-3' with a relative proportion of 92%. The  
195 corresponding synthetic yields (percentage of (+)-catechin that was converted into these  
196 glycosylated products) was 26% and 82% respectively. These results clearly indicate that these  
197 two variants are highly regioselective with respect to their transglycosylation activities on (+)-  
198 catechin.

### 199 3.4. Structural insights into the regioselectivity of AmSP-P140D and AmSP-Q353F

200 To further understand the observed regioselectivities, we performed molecular docking  
201 simulations with several conformations of the glucosyl intermediate of AmSP-Q353F and AmSP-  
202 P140D. The preferred orientations of various (+)-catechin conformers in the acceptor site of the  
203 glucosyl-enzyme intermediate were assessed using docking protocols implemented in Autodock  
204 Vina. Docking poses were filtered for reactivity, by considering those with an oxygen of (+)-  
205 catechin within 3 Å of the C1 atom of the glucosyl moiety as productive. Docking results were  
206 consistent with the observed experimental regioselectivity. For AmSP-Q353F, productive poses for  
207 glucosylation of (+)-catechin in OH3' position is overwhelmingly favoured energetically when

208 compared to the other hydroxyl groups (OH-4', OH-5 and in position 7) of the flavonoid (Figure  
209 S6). On the other hand, for *AmSP-P140D*, the most favoured productive poses for glucosylation of  
210 (+)-catechin is on OH-4' position (Figures S6). Comparison of the binding energies of the  
211 productive poses of (+)-catechin towards OH-3' and OH-4' glucosylation provided in Figure 3A  
212 clearly explains the observed regioselectivity. For each enzyme, structural analysis of the best  
213 productive poses showed a distance of 3.0 Å between the C1 atom of the glucosyl moiety and the  
214 OH-3' or OH-4' of (+)-catechin, and a distance with D203 residue of 4.0 Å (Figure 3B and 3C). For  
215 *AmSP-P140D*, (+)-catechin is stabilized in the active +1 site by a network of 4 hydrogen bonds and  
216 numerous hydrophobic contacts (Figure 4).

#### 217 4. Discussion

218 In glycochemistry, the fine control of the regioselectivity is the Holy Grail in enzymatic reactions  
219 catalysed by glycosyl hydrolase (GHs) such as sucrose phosphorylase. A disadvantage of GHs is  
220 their moderate regioselectivity, meaning that a mixture of products is often formed when the  
221 acceptor contains more than one hydroxyl group. Previously, for (+)-catechin which consists of five  
222 phenolic hydroxyl groups, we generated with *BaSP-Q345F* and *BaSP-P134D/Q345F* a mixture of  
223 glucosylated regioisomers: CAT-3', CAT-5 and CAT-3',5 with a ratio of 51:25:24 for *BaSP-Q345F* and  
224 82:9:9 for *BaSP-P134D/Q345F*. Another drawback is the relatively low product yields. With the  
225 same variants, we obtained a synthetic yield of 34%/15%/9% and 40%/5%/4%, respectively. In the  
226 active site of the SPs, the -1 site is rigid to allow a high selectivity on glucose while the +1 site is  
227 more flexible and can accept several types of acceptors or leaving groups. The +1 site of *AmSP-WT*,  
228 is mainly shaped by two highly labile loops, loop A (<sup>344</sup>AAASNLDLYQ<sup>353</sup>) and loop B (<sup>138</sup>FRPRP<sup>142</sup>),  
229 which undergo crucial conformational changes throughout the catalytic cycle suited for binding  
230 either fructose or phosphate. Crystal structure of *AmSP-WT* shows a wide access channel capable  
231 of accommodating naturally large polyphenolic acceptors. By site-directed mutagenesis, we

232 substituted the residue Q353 in loop B into F353 and/or the residue P140 into D140 in Loop A. We  
233 obtained three variants: *AmSP-P140D*, *AmSP-Q353F* and *AmSP-P140D/Q353F*. The double variant  
234 showed no improvement for the synthesis of CAT-3' with the obtainment of a mixture of products  
235 at 25°C (data not shown). By engineering the residue 353 of the active site, we enhanced the  
236 enzyme regioselectivity from a mixture of products to OH-3' position almost exclusively. Docking  
237 studies confirmed that the most favoured pose for (+)-catechin in the catalytic +1 site of *AmSP-*  
238 *Q353F* lead to the formation of CAT-3'. As seen with *BaSP-Q345F*, we hypothesized that the  
239 introduction of F353 as a potential partner for  $\pi$ - $\pi$  stacking leads to rearrangements in loop A with  
240 a shift of Y352 which can stabilise (+)-catechin in the active site by hydrophobic interactions. *BaSP-*  
241 *Q345F*, *BaSP-P134D/Q345F* and *AmSP-Q353F* preferentially glucosylate the OH-3' position of  
242 flavonoids while ignoring the OH-4' position. This was confirmed by docking simulations which  
243 highlighted that the most favoured pose for (+)-catechin in the catalytic site of *AmSP-Q353F*  
244 (Figure 3 and Table 2) would lead to the regioselective formation of CAT-3'. Surprisingly, while  
245 *BaSP-P140D* was not active, *AmSP-P140D* leads to the regioselective formation of CAT-4' (Figure 3  
246 and Table 2). Thus, switching Q353F mutation to P140D had shift completely the regioselectivity of  
247 *AmSP-WT* from CAT-3' to CAT-4'. An explanation enlightened by molecular modelling is the steric  
248 hindrance caused by F138/Y207/F217 residues between *AmSP-P140D* and the polyphenol rings  
249 (Figures 3B and S7). Indeed, we observed that the conformation of the acceptor site drastically  
250 changed and seems to allow only an almost linear orientation of all three (+)-catechin rings.  
251 Contrarily to *AmSP-Q353F*, those very strong constraints lead to the regioselective glucosylation of  
252 the OH-4' position of the flavonoid with a high proportion (89%).

## 253 5. Conclusion

254 In this study, we provided the first report of the use of variants of sucrose phosphorylase from  
255 *Alteromonas mediterranea* for the regioselective transglucosylation of (+)-catechin and the

256 synthesis of a novel compound fully characterized, (+)-catechin-4'-O- $\alpha$ -D-glucopyranoside (CAT-4').  
257 AmSP-Q353F and AmSP-P140D are able to synthesize regioselectively compound CAT-3' and CAT-  
258 4', with a proportion of 92% and 89%, respectively. With AmSP-P140D, we succeed to switch the  
259 regioselectivity from OH-3' to OH-4'-glucosylated (+)-catechin. Mutation P140D changes drastically  
260 the conformation of the acceptor site and seems to allow an almost linear alignment of the  
261 glucose moiety and of all three (+)-catechin rings allowing selectively the glucosylation of the  
262 position OH-4' of this flavonoid. Overall, the results described herein suggest that AmSP-Q353F  
263 and AmSP-P140D are suitable for the enzymatic regioselective synthesis of polyphenolic glucosides  
264 at high yields and could facilitate the synthesis of *de novo* products in OH-4' position using other  
265 phenolic phytochemicals such as quercetin or kaempferol.

## 266 **Supporting information**

267 For details about melting curves, kinetic parameters analysis, HPLC/MS, NMR spectra, etc., please  
268 see provided Electronic Supplementary Information.

## 269 **Author Contributions**

270 MG and MD wrote the original draft. MG, MD, CM, BO and JH developed the methodology. MG,  
271 MD, CS and EL performed the experimental investigation and the following analysis. DT and FF  
272 obtained the crystallographic structure of AmSP-WT. JH and BO performed the molecular and  
273 docking simulations and the following analysis. CM obtained the funding, designed and directed  
274 the project. All authors discussed the results and contributed to the final manuscript.

## 275 **Conflicts of interest**

276 There are no conflicts to declare.

## 277 Acknowledgments

278 MG post-doctoral fellowship was supported by the “Region Pays de la Loire” and “Université  
279 Bretagne Loire” within the project “FunRégiOx”, and MD thesis by “Nantes Université”. We thank  
280 the CEISAM NMR platform for the NMR experiments.

## 281 References

- 282 [1] A. Beygmoradi, A. Homaei, R. Hemmati, Marine chitinolytic enzymes, a biotechnological  
283 treasure hidden in the ocean?, *Appl. Microbiol. Biotechnol.* 102 (2018) 9937–9948.  
284 <https://doi.org/10.1007/s00253-018-9385-7>
- 285 [2] V.S. Bernan, M. Greenstein, M.W. Maiese, Marine microorganisms as a source of new  
286 natural products, *Adv. Appl. Microbiol.* 43 (1997) 57-90. [https://doi.org/10.1016/s0065-](https://doi.org/10.1016/s0065-2164(08)70223-5)  
287 [2164\(08\)70223-5](https://doi.org/10.1016/s0065-2164(08)70223-5).
- 288 [3] H. Harmsen, D. Prieur, C. Jeanthon, Distribution of microorganisms in deep-sea  
289 hydrothermal vent chimneys investigated by whole-cell hybridization and enrichment  
290 culture of thermophilic subpopulations, *Appl. Environ. Microbiol.* 63 (1997) 2876-2883.  
291 <https://doi.org/10.1128/aem.63.7.2876-2883.1997>.
- 292 [4] T.H. Cheng, N. Ismail, N. Kamaruding, Industrial enzymes-producing marine bacteria from  
293 marine resources, *Biotechnology Reports.* 27 (2020) e00482.  
294 <https://doi.org/10.1016/j.btre.2020.e00482>.
- 295 [5] M. Kraus, J. Görl, M. Timm, Synthesis of the rare disaccharide nigerose by structure-based  
296 design of a phosphorylase mutant with altered regioselectivity, *ChemComm* 52 (2016)  
297 4625–4627. <https://doi.org/10.1039/c6cc00934d>.

- 298 [6] J. Franceus et al., “Rational design of an improved transglucosylase for production of the  
299 rare sugar nigerose, ChemComm. 55 (2019) 4531–4533.  
300 <https://doi.org/10.1039/c9cc01587f>.
- 301 [7] M. Kraus, C. Grimm, J. Seibel, Redesign of the Active Site of Sucrose Phosphorylase through  
302 a Clash-Induced Cascade of Loop Shifts, ChemBioChem 17 (2016) 33–36.  
303 <https://doi.org/10.1002/cbic.201500514>.
- 304 [8] M. Kraus, C. Grimm, J. Seibel, “Switching enzyme specificity from phosphate to resveratrol  
305 glucosylation, ChemComm. 53 (2017) 12181–12184. <https://doi.org/10.1039/c7cc05993k>.
- 306 [9] D. Aerts, T. F. Verhaeghe, B. I. Roman, Transglucosylation potential of six sucrose  
307 phosphorylases toward different classes of acceptors, Carbohydr. Res. 346 (2011) 1860-  
308 1867. <https://doi.org/10.1016/j.carres.2011.06.024>.
- 309 [10] M. Demonceaux, M. Goux, M., J. Hendrickx, Regioselective glucosylation of (+)-  
310 catechin using a new variant of the sucrose phosphorylase from *Bifidobacterium*  
311 *adolescentis*, Org. Biomol. Chem. 11 (2023). <https://doi.org/10.1039/d3ob00191a>.
- 312 [11] D. Sprogoe, L.A.M. van den Broek, O. Mirza, Crystal structure of sucrose  
313 phosphorylase from *Bifidobacterium adolescentis*, Biochemistry 43 (2004) 1156-1162.  
314 <https://doi.org/10.1021/bi0356395>.
- 315 [12] M. E. Dirks-Hofmeister, T. Verhaeghe, K. De Winter, Creating Space for Large  
316 Acceptors: Rational Biocatalyst Design for Resveratrol Glycosylation in an Aqueous System,  
317 Angew. Chemie. 54 (2015) 9289–9292. <https://doi.org/10.1002/anie.201503605>.
- 318 [13] S. Kitao, T. Ariga, T. Matsudo, The Syntheses of Catechin-glucosides by  
319 Transglycosylation with *Leuconostoc Mesenteroides* Sucrose Phosphorylase, Biosci.  
320 Biotechnol. Biochem. 57 (1993). 2010–2015, 1993, <https://doi.org/10.1271/bbb.57.2010>.
- 321 [14] K. De Winter, G. Dewitte, M.E. Dirks-Hofmeister, Enzymatic Glycosylation of  
322 Phenolic Antioxidants: Phosphorylase-Mediated Synthesis and Characterization, Journal of

- 323 Agricultural and Food Chemistry 2015 63 (46) 10131-10139.  
324 <https://doi.org/10.1021/acs.jafc.5b04380>
- 325 [15] K. De Winter, A. Cerdobbel, W. Operational stability of immobilized sucrose  
326 phosphorylase: continuous production of  $\alpha$ -glucose-1-phosphate at elevated  
327 temperatures. Process Biochem. 46 (2011) 1074–1078.  
328 <https://doi.org/10.1016/j.procbio.2011.08.002>.
- 329 [16] J. Franceus, T. Desmet, Sucrose Phosphorylase and Related Enzymes in Glycoside  
330 Hydrolase Family 13: Discovery, Application and Engineering, Int. J. Mol. Sci. 21 (2020)  
331 2526. <https://doi.org/10.3390/ijms21072526>
- 332 [17] A. López-López, S.G. Bartual, L. Stal, Genetic analysis of housekeeping genes reveals  
333 a deep-sea ecotype of *Alteromonas macleodii* in the Mediterranean Sea, Environ Microbiol.  
334 7 (2005)649-659. <https://doi.org/10.1111/j.1462-2920.2005.00733.x>
- 335 [18] E.P. Ivanova, M. López-Pérez, M. Zabalos, Ecophysiological diversity of a novel  
336 member of the genus *Alteromonas*, and description of *Alteromonas mediterranea* sp. nov.  
337 Antonie Van Leeuwenhoek. 107 (2015) 119-132. [https://doi.org/10.1007/s10482-014-](https://doi.org/10.1007/s10482-014-0309-y)  
338 [0309-y](https://doi.org/10.1007/s10482-014-0309-y)
- 339 [19] M. López-Pérez, A. Gonzaga, A.B. Martín-Cuadrado, Genomes of surface isolates of  
340 *Alteromonas macleodii*: the life of a widespread marine opportunistic copiotroph. Sci Rep  
341 2, 696 (2012). <https://doi.org/10.1038/srep00696>
- 342 [20] O. Mirza, L.K. Skov, D. Sprogø, Structural Rearrangements of Sucrose  
343 Phosphorylase from *Bifidobacterium adolescentis* during Sucrose Conversion, J. Biol. Chem.  
344 281 (2006) 35576-35584. <https://doi.org/10.1074/jbc.M605611200>.
- 345 [21] T. Verhaeghe, M. Diricks, D., Mapping the acceptor site of sucrose phosphorylase  
346 from *Bifidobacterium adolescentis* by alanine scanning, J. Mol. Catal 96 (2013) 81-88.  
347 <https://doi.org/10.1016/j.molcatb.2013.06.014>

- 348 [22] C. A. Rohl, C.E. Strauss, K.M. Misura, Protein structure prediction using Rosetta,  
349 Methods Enzymol. 383 (2004) 66–93. [https://doi.org/10.1016/S0076-6879\(04\)83004-0](https://doi.org/10.1016/S0076-6879(04)83004-0)
- 350 [23] R. Schumacker and S. Tomek, Understanding Statistics Using R, Springer, 2013.  
351 <https://doi.org/10.1007/978-1-4614-6227-9>
- 352 [24] R. A. Laskowski, M. B. Swindells, LigPlot+: multiple ligand-protein interaction  
353 diagrams for drug discovery. J. Chem. Inf. Model., 51 (2011) 2778-2786.  
354 <https://doi.org/10.1021/ci200227u>
- 355



356 **Figures caption and legend**

357

358 **Figure 1: Crystallographic structures of *Ba*SP-WT and *Am*SP-WT focused on residues involved in**

359 **(A) sucrose and (B) fructose binding. (A)** In magenta: Loop A (in sticks for *Ba*SP-WT: Y344/D342, in

360 sticks for *Am*SP-WT: Y352/D350); orange: Loop B (in sticks for *Ba*SP-WT: R135, in sticks for *Am*SP-

361 WT: R141); and blue: residues of the catalytic triad (in sticks for *Ba*SP-WT: D192/E232/D290, in

362 sticks for *Am*SP-WT: D203/E243/D301). **(B)** In magenta: Loop A (in sticks for *Ba*SP-WT:

363 D342/L343/Y344/Q345, in sticks for *Am*SP-WT: D350/L351/Y352/Q353); orange: Loop B (in sticks

364 for *Ba*SP-WT: Y132/R133/P134/R135, in sticks for *Am*SP-WT: F138/R139/P140/R141); Cyan:

365 residues involved in sucrose phosphorylase activity (in sticks for *Ba*SP-WT: Y196/V233/H234, in

366 sticks for *Am*SP-WT: Y207/I244/H245).

367

368 **Figure 2: Products profile of *Am*SP-Q353F and *Am*SP-P140D using (+)-catechin as acceptor.**

369 Proportion of each regioisomers was calculated from the area under the curves obtained by

370 analytical HPLC (isocratic mode at 80% H<sub>2</sub>O (v/v), 0.1% formic acid (v/v) and 20% MeOH (v/v), 0.1%

371 formic acid (v/v)).

372

373 **Figure 3: Structural rearrangement of *Am*SP active site and best productive poses of (+)-catechin**

374 **towards OH-3' and OH-4' for *Am*SP-P140D (B) and *Am*SP-Q353F (C) glucosyl-enzyme. (A)**

375 Comparison of binding energy of productive poses of (+)-catechin towards OH-3' and OH-4' for

376 *Am*SP-P140D and *Am*SP-Q353F glucosyl-enzyme ( $\Delta G = -9.3$  kcal/mol for *Am*SP-Q353F and  $-9.2$

377 kcal/mol for *Am*SP-P140D). In magenta: Loop A with in sticks Y352/D350/Q(F)353 residues;

378 orange: Loop B with in sticks R141/F138 and D140 for *Am*SP-P140D; blue: residues of the catalytic

379 triad with in sticks D203/D301/DGC243; and pink : (+)-catechin.

380 **Figure 4. Analysis of the interaction between (+)-catechin and AmSP-P140D.** Shown are hydrogen  
381 bonds and hydrophobic contacts between the (+)-catechin substrate (denoted Kxn1) and the  
382 interacting residues including the glucosylated-aspartyl (Dgc203). The diagram was obtained using  
383 LigPlot Plus v.2.2 [24].

384

385

386 **Table 1: Apparent kinetic parameters for sucrose hydrolysis by AmSP and its variants.** Reactions

387 were conducted in MOPS 50 mM pH 8.0 at 25°C with or without 20% of DMSO. Values are based

388 on Michaelis-Menten fittings obtained with Microsoft Excel. Hanes-Woolf plots are included in the

389 electronic supplementary information (Figures S3 and S4).

	0% DMSO			20% DMSO		
	$K_M$ (mM)	$k_{cat}$ ( $s^{-1}$ )	$k_{cat}/K_M$	$K_M$ (mM)	$k_{cat}$ ( $s^{-1}$ )	$k_{cat}/K_M$
<b>AmSP-WT</b>	$0.8 \pm 0.2$	$120 \pm 34$	$156.6 \pm 26.2$	$0.91 \pm 0.1$	$109 \pm 12$	$124.6 \pm 7.6$
<b>AmSP-P140D</b>	$1.8 \pm 0.5$	$13 \pm 2.0$	$7.34 \pm 1.4$	$1.02 \pm 0.4$	$19 \pm 4.0$	$20.12 \pm 7.1$
<b>AmSP-Q353F</b>	$4.6 \pm 1.2$	$2 \pm 0.0$	$0.46 \pm 0.1$	$4.23 \pm 0.8$	$3 \pm 0.0$	$0.79 \pm 0.1$

390

391

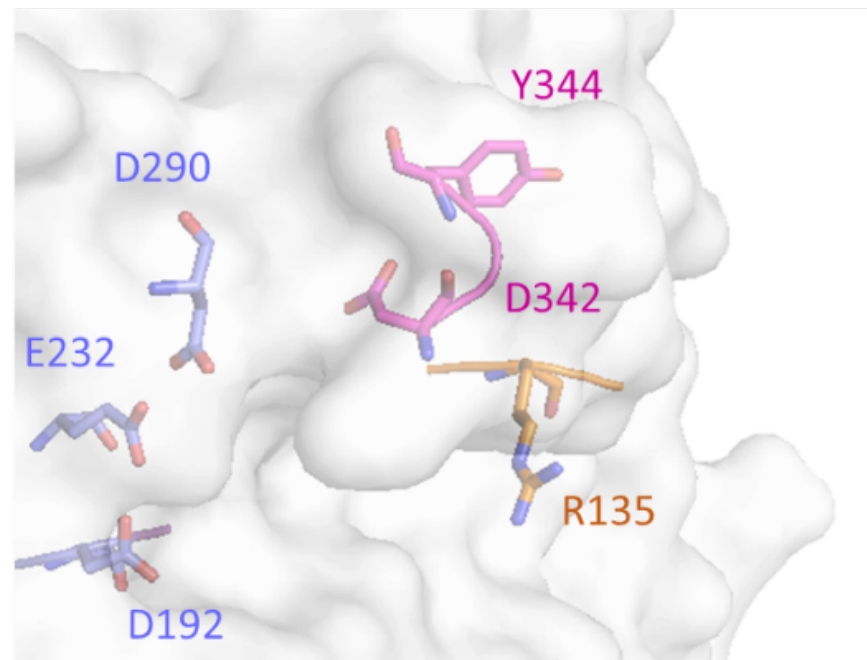
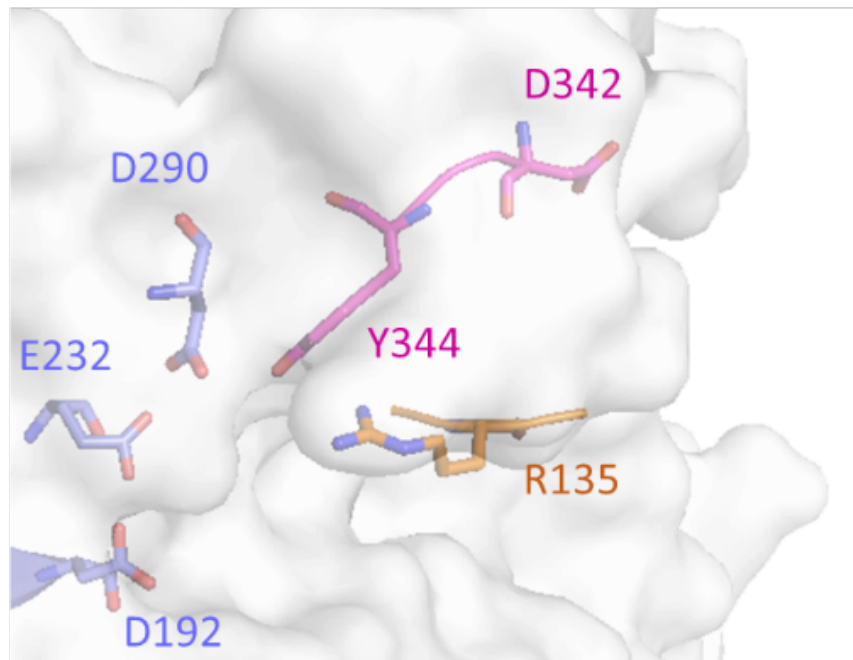
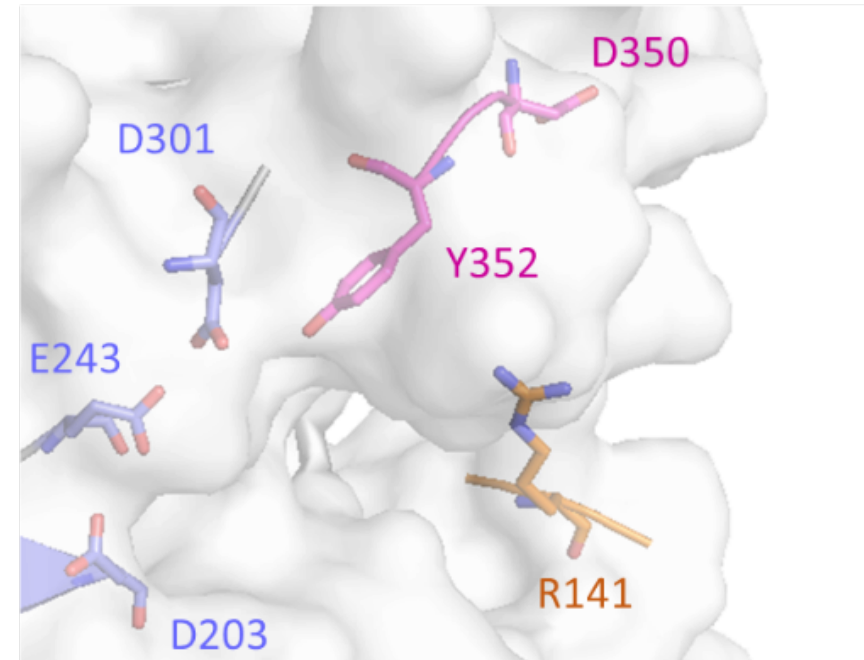
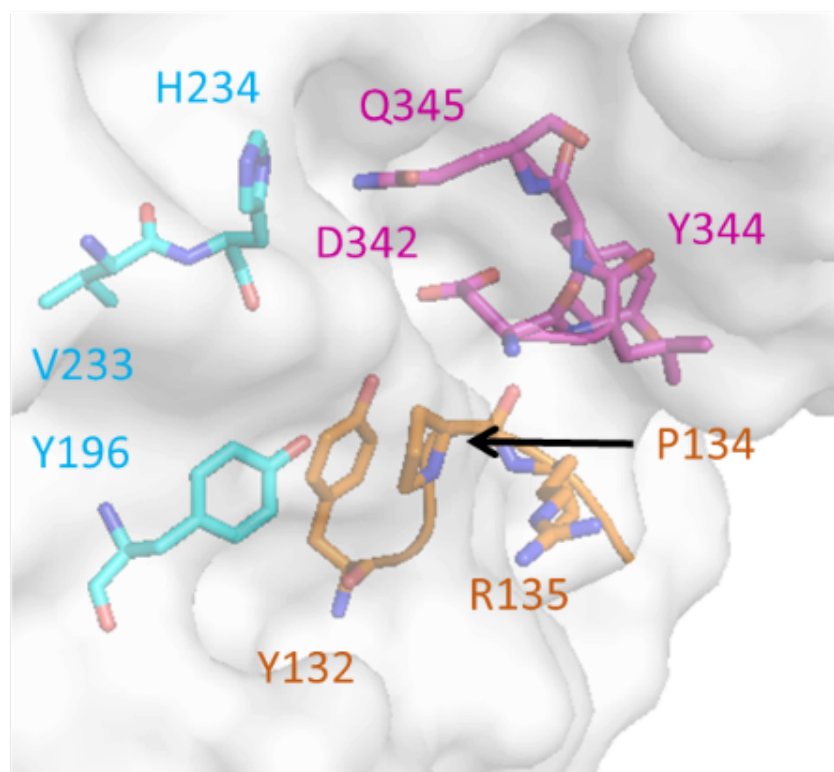
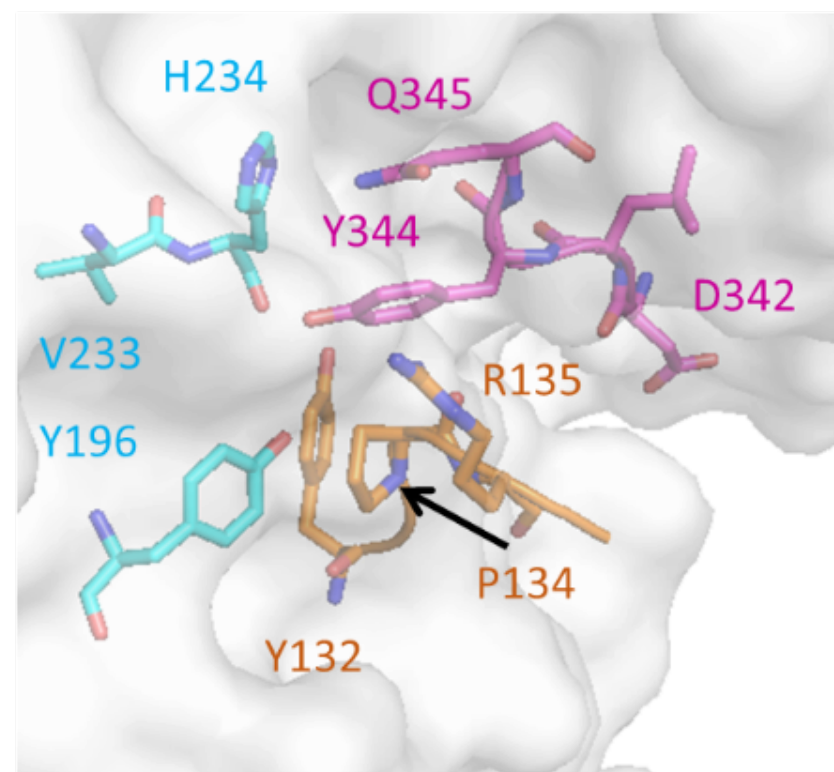
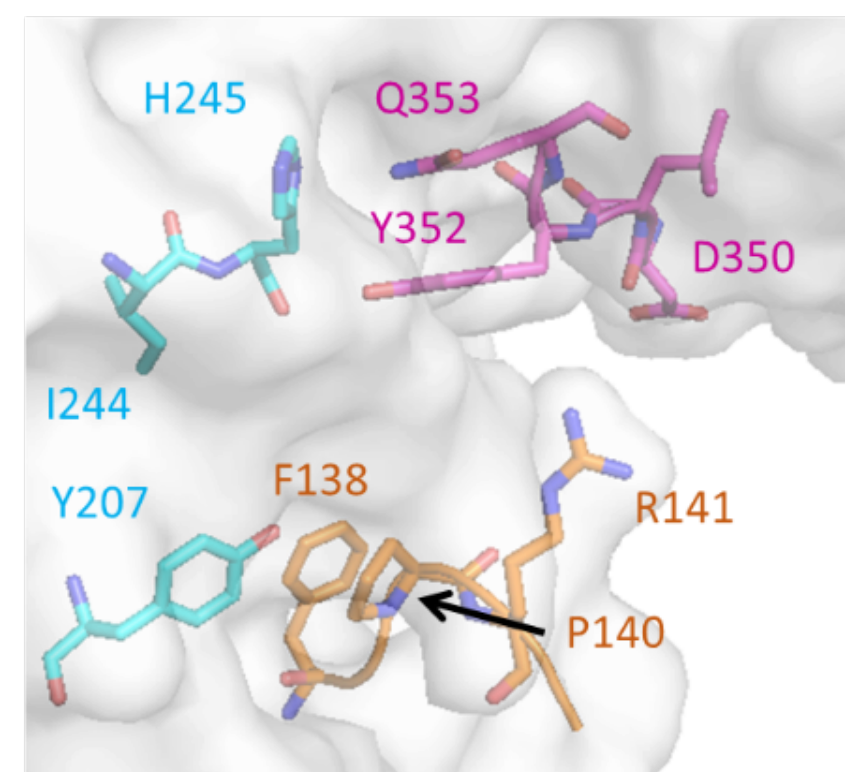
392 **Table 2: Synthetic yields (A) and relative proportion (B) of (+)-catechin glycosylated products**  
393 **obtained with P140D and Q353F variants of AmSP.** Synthetic yields are expressed as a percentage  
394 of (+)-catechin that was converted into the corresponding glycosylated products (CAT-4': (+)-  
395 catechin-4'-O- $\alpha$ -D-glucopyranoside; CAT-3': (+)-catechin-3'-O- $\alpha$ -D-glucopyranoside; CAT-5: (+)-  
396 catechin-5-O- $\alpha$ -D-glucopyranoside; CAT3',5: (+)-catechin-3',5-O- $\alpha$ -D-diglucopyranoside). The  
397 relative proportion of each product was calculated from the area under the curves obtained by  
398 analytical HPLC at 24 h with the same conditions than for Figure S5.

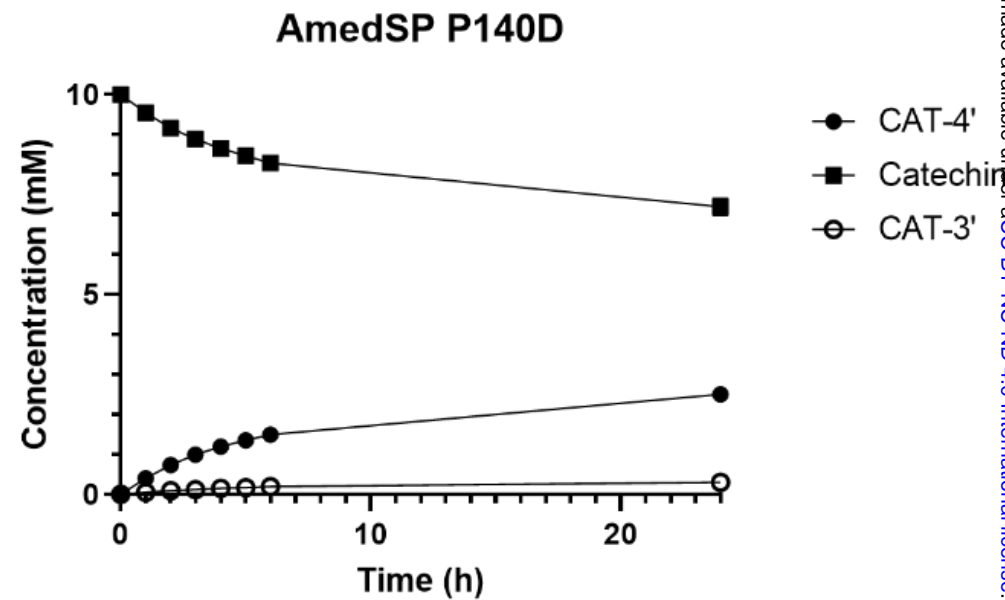
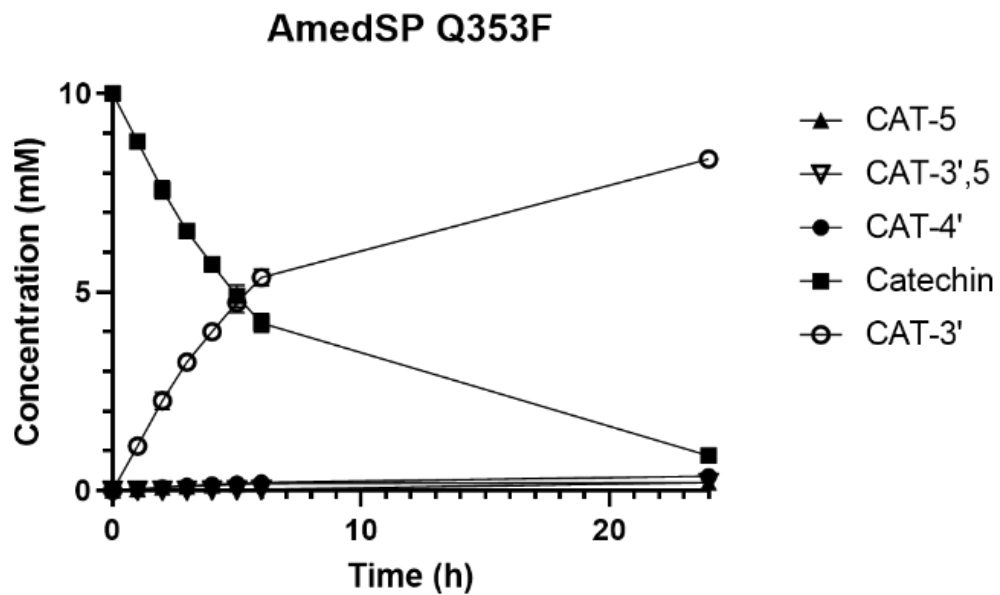
Product	Synthetic yields				Proportion of each product			
	CAT-4'	CAT-3'	CAT-5	CAT-3',5	CAT-4'	CAT-3'	CAT-5	CAT-3',5
P140D	26.36%	3.21%	Traces	Traces	89.08%	10.92%	Traces	Traces
Q353F	3.49%	82.64%	2.22%	1.85%	3.93%	91.58%	2.28%	2.21%

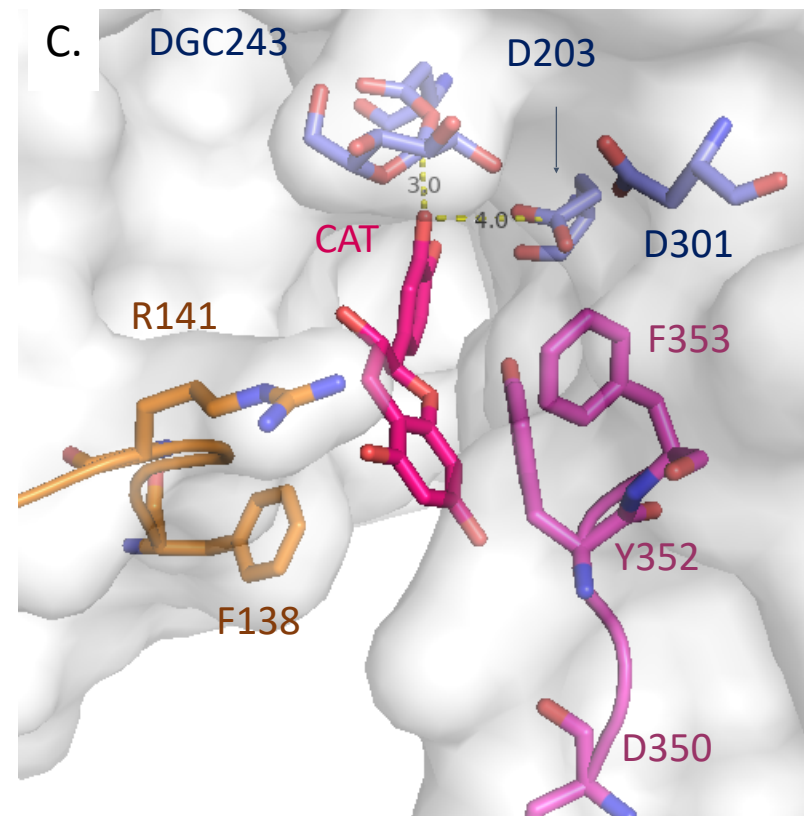
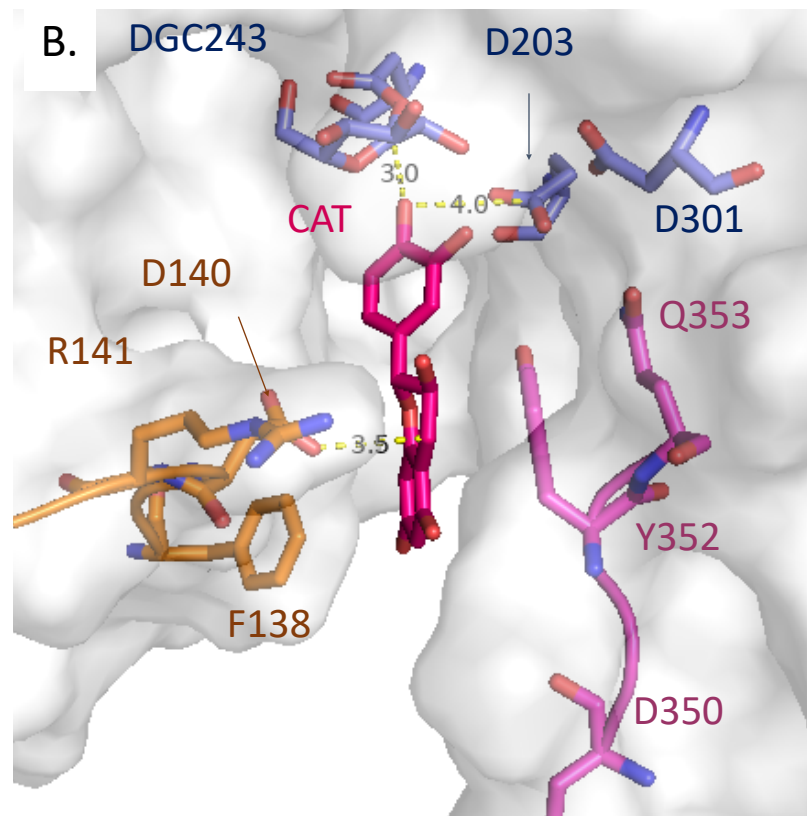
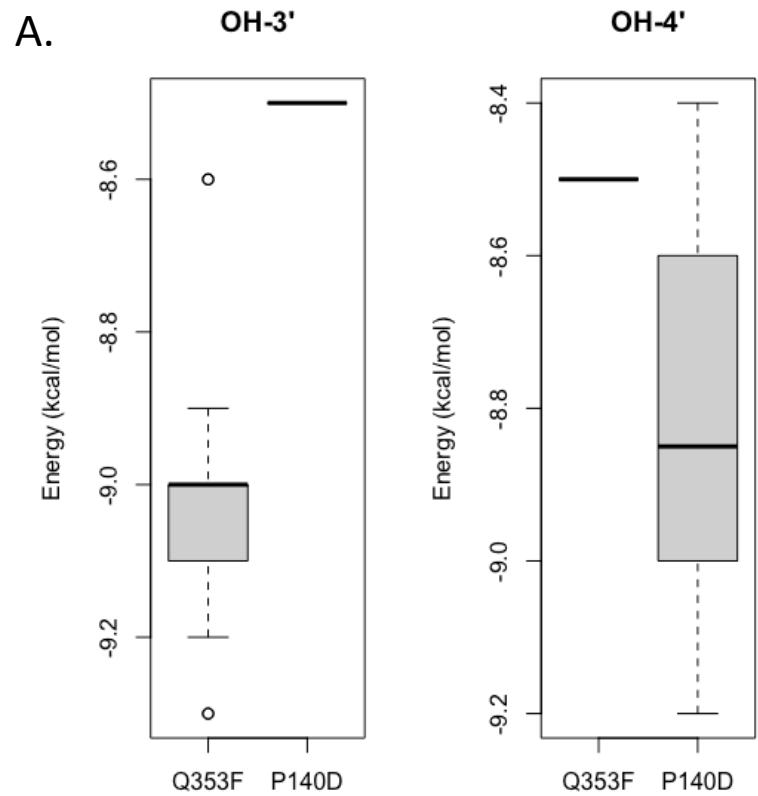
399

400

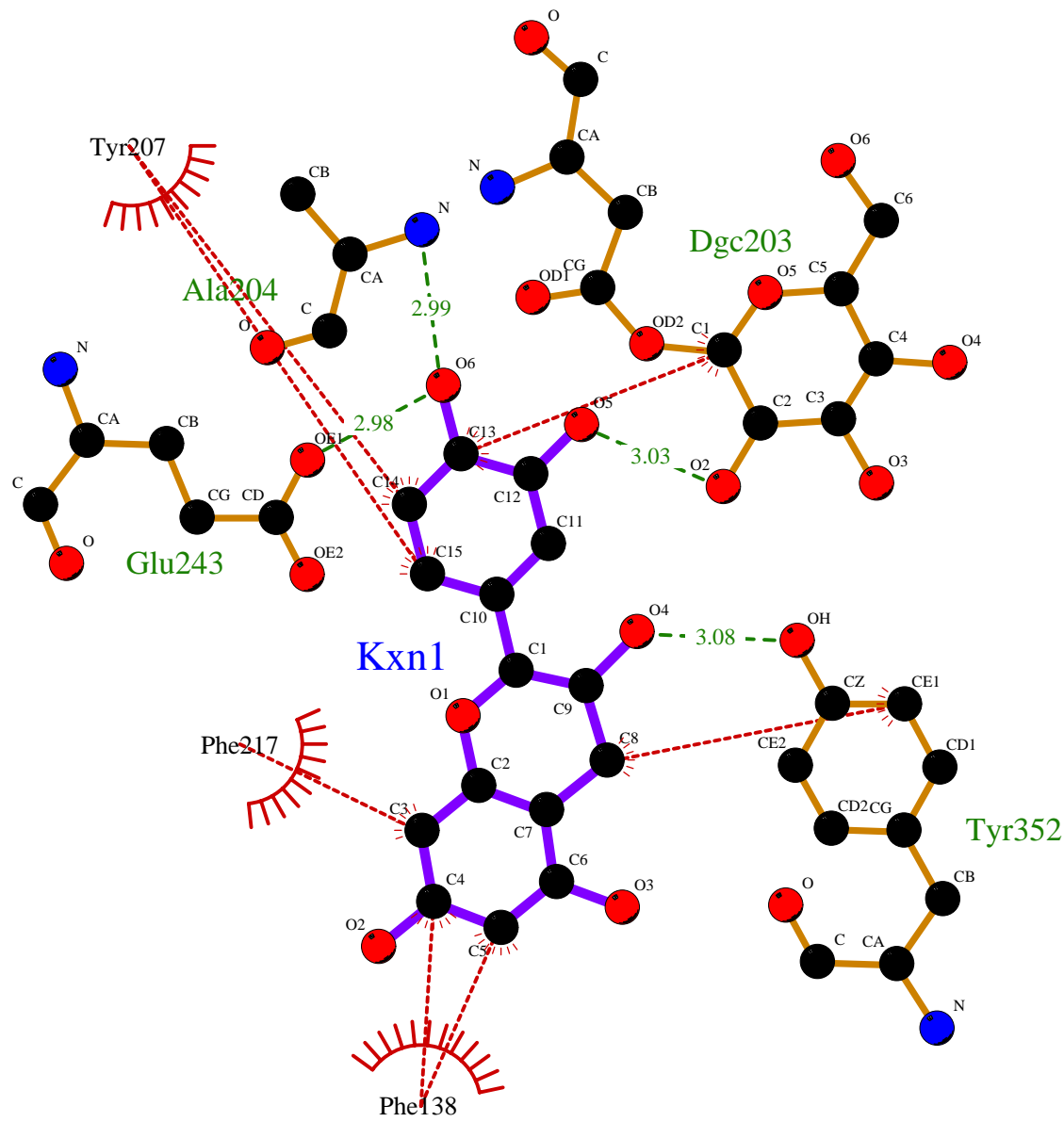
401

**A.****BaSP WT  
(1R7A)****BaSP WT  
(2GDV.B)****AmSP WT  
(7ZNP)****B.****BaSP WT  
(1R7A)****BaSP WT  
(2GDV.B)****AmSP WT  
(7ZNP)**









## Key:



Ligand bond



Non-ligand bond



Hydrogen bond and its length



His 53 Non-ligand residues involved in hydrophobic contact(s)



Corresponding atoms involved in hydrophobic contact(s)